Detailed Molecular Dynamics Simulations of a Model NaPSS in Water

Jan-Michael Y. Carrillo and Andrey V. Dobrynin*

Polymer Program, Institute of Materials Science and Department of Physics, University of Connecticut, Storrs, Connecticut 06269

Received: March 4, 2010; Revised Manuscript Received: June 15, 2010

Hydrophobic polyelectrolytes are known to form necklace-like structures of dense beads connected by strings of monomers. This structure appears as a result of optimization of the electrostatic and short-range interactions. To elucidate the effect of counterion condensation and solvent on polyelectrolyte conformations, we performed two sets of molecular dynamics simulations of model poly(styrene)-*co*-styrene sodium sulfonate (NaPSS) chains with the degree of polymerization $N = 16-64$ and fraction of charged monomers $f = 0.25-1$ in aqueous solutions: (1) water molecules were considered explicitly using the TIP3P-PME model and (2) water molecules were modeled as a dielectric continuum with the dielectric constant 77.73. Our simulations showed that with increasing fraction of sulfonated groups f a polystyrene sulfonate chain adopts an elongated conformation. There is a transition between collapsed and elongated states which is manifested in the change of the scaling dependence of the chain size on the degree of polymerization. The effect of the water−ion interactions on counterion condensation was analyzed by comparing the radial distribution functions between the sulfonated groups and counterions for chains with different f values. In the case of the collapsed NaPSS chains, it was found that ionized groups are located at the globular surface.

1. Introduction

Polyelectrolytes are polymers with ionizable groups.[1−7] In polar solvents such as water, these groups can dissociate, leaving charges on polymer chains and releasing counterions in solution. Examples of polyelectrolytes include sodium polystyrene sulfonate, polyacrylic and polymethacrylic acids and their salts, DNA, and other polyacids and polybases. Electrostatic interactions between charges lead to the rich behavior of polyelectrolyte solutions which is qualitatively different from those of uncharged polymers.[8−10]

The structure of polyelectrolyte chains in solution is determined by a fine interplay between electrostatic interactions between ionized groups and the interactions of the polymer backbone with the surrounding solvent. For many polyelectrolytes water is a poor solvent for the polymer backbone, corresponding to an effective attraction between monomers. This attraction causes neutral polymer chains without charged groups to collapse into spherical globules in order to maximize the number of favorable polymer−polymer contacts.[8,9] Polymeric globules change their shape and size upon charging. This phenomenon was first discovered by Katchalsky and Eisenberg[11] in their study of the viscosity of aqueous solutions of poly(methacrylic acid) PMA. The viscosity of dilute PMA solutions stayed almost constant at low solution pH and then abruptly increased as solution pH reached some critical value, indicating a dramatic change in the chain dimensions.

It is interesting to point out that the problem of the stability of a charged globule is similar to the classical problem of the instability of a charged droplet, considered by Lord Rayleigh.[11] The Rayleigh experiments had shown that a charged droplet is unstable and breaks into smaller droplets if its charge exceeds a critical value. A polyelectrolyte chain in a poor solvent reduces its energy in a way similar to a charged droplet by splitting into a set of smaller charged globules, called beads. Since this transformation occurs in a single chain, all these beads are connected by strings of monomers into a necklace of globules.[12] This necklace model of a polyelectrolyte chain in a poor solvent was proposed by Dobrynin, Rubinstein, and Obukhov.[12] The Monte Carlo simulations of a freely jointed uniformly charged polyelectrolyte chain with fractional charge f on each monomer[12] have demonstrated that in a poor solvent for a polymer backbone there is a cascade of transitions between necklaces with different number of beads as charge on the chain increases.

The full domain of stability of necklace globules in the solvent quality/salt concentration plane was investigated by Monte Carlo[13] and by molecular dynamics simulations.[14] With increasing salt concentration the necklaces transform into elliptical globules. These results of computer simulations are in good qualitative agreement with models of a polyelectrolyte chain in a poor solvent.[12,15−19]

The necklace structure of polyelectrolyte chains in poor solvents was confirmed by small-angle neutron scattering (SANS) experiments[20] in dilute solutions of water/acetone mixtures of poly(methacryloylethyltrimethylammonium methyl sulfate), by NMR spectra[21] of semidilute solutions of poly(styrenesulfonic acid), poly(methacrylic acid) (PMA), and poly(acrylic acid) (PAA) in water/methanol mixtures, and by atomic force microscopic (AFM) images of poly(2-vinylpyridine) and poly(methacryloyloxyethyl dimethylbenzylammonium chloride) adsorbed at mica surfaces.[27,28]

It was reported by Essafi[22,23] that the exponent, α, of the power law concentration dependence of the solution correlation length $\xi(c) \sim c^{\alpha}$ varies with the degree of sulfonation of NaPSS. For example, this exponent was $\alpha = -0.38$ for 40% sulfonation throughout the whole semidilute solution regime while it was close to the classical value $\alpha = -0.5$ for the fully sulfonated samples. Similar observations were reported by Heitz et al.[24] for poly(methacrylic acid) in water as a function of its neutralization. The exponent α of the concentration dependence of the correlation length was found to change from −0.43 to −0.31 as the neutralization decreased from 0.95 to 0.09. The

10.1021/jp101978k © 2010 American Chemical Society
Published on Web 07/06/2010

TABLE 1: System Sizes and Densities for NVT Simulations

Simulations with Explicit Water								
f	f_a	N	L_x, L_y, L_z (Å)	volume (Å^3)	n_{water}	n_{atoms}	n_{Na}	ρ_{box} (g/cm^3)
1	1.000	16	30.54	28 485	889	2 940	16	1.13
1/2	0.500	16	30.54	28 476	889	2 908	8	1.08
1/3	0.375	16	30.40	28 086	889	2 900	6	1.08
1/4	0.294	17	30.99	29 775	944	3 074	5	1.08
1/2	0.515	33	38.78	58 341	1833	5 997	17	1.09
1/3	0.355	31	37.85	54 242	1722	5 614	11	1.08
1/4	0.273	33	38.59	57 459	1833	5 965	9	1.08
1/2	0.512	41	41.58	71 877	2278	7 452	21	1.10
1/2	0.510	49	44.00	85 184	2722	8 904	25	1.11
1/2	0.509	57	46.51	100 595	3167	10 359	29	1.09
1/2	0.508	65	48.43	113 582	3611	11 811	33	1.10
1/3	0.344	64	48.20	111 969	3556	11 589	22	1.08
1/4	0.262	65	48.35	113 051	3611	11 747	17	1.08
Simulations in a Dielectric Medium with Dielectric Constant $\varepsilon = 77.73$								
f	f_a	N	L_x, L_y, L_z (Å)	volume (Å^3)	n_{water}	n_{atoms}	n_{Na}	$\rho_{monomer}$ (Å^{-3})
1	1.000	16	30.54	28 485	0	273	16	6×10^{-4}
1/2	0.500	16	30.54	28 476	0	241	8	6×10^{-4}
1/3	0.375	16	30.40	28 086	0	233	6	6×10^{-4}
1/4	0.294	17	30.99	29 775	0	242	5	6×10^{-4}
1/2	0.515	33	38.78	58 341	0	498	17	6×10^{-4}
1/3	0.355	31	37.85	54 242	0	448	11	6×10^{-4}
1/4	0.273	33	38.59	57 459	0	466	9	6×10^{-4}
1/2	0.508	65	48.43	113 582	0	978	33	6×10^{-4}
1/3	0.344	64	48.20	111 969	0	921	22	6×10^{-4}
1/4	0.262	65	48.35	113 051	0	914	17	6×10^{-4}
1	1.000	16	125.99	2 000 000	0	273	16	8×10^{-6}
1	1.000	24	144.26	3 000 000	0	409	24	8×10^{-6}
1	1.000	32	158.74	4 000 000	0	545	32	8×10^{-6}
1/2	0.500	16	125.99	2 000 000	0	241	8	8×10^{-6}
1/2	0.500	24	144.26	3 000 000	0	361	12	8×10^{-6}
1/2	0.500	32	158.74	4 000 000	0	481	16	8×10^{-6}
1/2	0.500	40	171.00	5 000 000	0	601	20	8×10^{-6}
1/2	0.500	48	181.71	6 000 000	0	721	24	8×10^{-6}
1/2	0.500	56	191.29	7 000 000	0	841	28	8×10^{-6}
1/2	0.500	64	200.00	8 000 000	0	961	32	8×10^{-6}

evolution of the polyelectrolyte solution with increasing polymer concentration in solvophobic polyelectrolytes in a series of polar organic solvents[25] shows that the scaling exponent α of the concentration dependence of the correlation length changes from -0.45 to -0.13. The analysis of the bead structure was reported by Williams' group.[26,27] The conductivity measurements by Bordi et al.[28] are also in agreement with the necklace structure of the hydrophobic polyelectrolytes.

Molecular dynamics simulations of partially charged polyelectrolytes with explicit counterions in poor solvent conditions were performed by the German group[29−33] and by Liao et al.[34] These simulations have shown that polyelectrolyte chains at low polymer concentrations form necklaces of beads connected by strings. The fraction of condensed counterions on the chain increases with increasing polymer concentration, causing the chain size to decrease by decreasing the length of strings and the number of beads per chain. At even higher polymer concentrations, polymer chains form a concentrated polyelectrolyte solution. In this range of polymer concentrations the chain size is observed to increase toward its Gaussian value.[18] However, at finite polymer concentrations the necklace stability region is strongly influenced by the counterion condensation such that polyelectrolyte chains adopt necklace-like conformation only in the narrow range of the interaction parameters.[31−36]

The concentration dependence of the fraction of "free" counterions in salt-free solutions of poly(styrene)-*co*-styrene sodium sulfonate (NaPSS) was recently measured by Essafi et al.[37] Using osmotic pressure measurements and cryoscopy, they have found that the fraction of ionized groups on NaPSS is significantly lower in comparison with the theoretically expected value[18] and with the measured one for a hydrophilic polyelectrolyte, sodium-2-acrylamide-2-methylpropane sulfonate (AMAMPS). For the hydrophilic polyelectrolyte AMAMPS, the fraction of ionized groups on the polymer backbone corresponding to the fraction of released (free) counterions stays almost constant at about $f_{eff} = 0.34$ for the bare (chemical) charge fractions $f = 0.95$ and 0.64 throughout the polymer concentration range from 0.01 to 0.1 M. (Note that in this concentration range the osmotic pressure is dominated by free counterions.) It slightly decreases toward $f_{eff} = 0.115$ for $f = 0.51$ and reaches 0.15 at $f = 0.4$. This behavior of hydrophilic polyelectrolytes is in surprisingly good agreement with the Manning−Oosawa condensation theory[1,38,39] showing saturation of f_{eff} when the chemical charge fraction f exceeds a critical value. A qualitatively different behavior is observed for hydrophobic polyelectrolytes. For these polyelectrolytes the fraction of free counterions f_{eff} decreases linearly with decreasing the bare charge fraction f in the whole range independent of the chain degree of polymerization, N. Only for the fully charged chains with $f = 1$ the fraction of ionized groups reaches the saturation value predicted by the Manning−Oosawa condensation theory[1,38,39] and is close to the saturation value observed for hydrophilic polyelectrolyte AMAMPS. The fraction of free counterions f_{eff} approaches zero at a value f on the order of 0.18, which is close

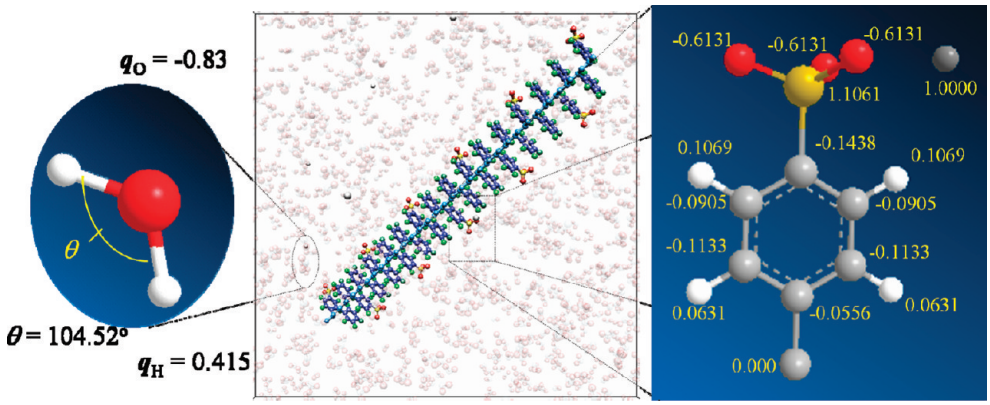

Figure 1. Snapshot of a polystyrene sulfonate chain with the fraction of charged monomers $f = 1/4$ (center). Sulfonated styrene group with all atomistic details and partial charge distribution is shown on the right, and the water molecule is shown on the left.

to the limit of solubility for NaPSS in water. Thus, the counterion condensation in solutions of hydrophobic polyelectrolytes occurs in a qualitatively different way than in solutions of hydrophilic polyelectrolytes.

The strong correlation between the decrease in the fraction of ionized groups with the fluorescence emission ratio I_1/I_3 for pyrene observed in salt-free NaPSS solutions indicates that the unusual counterion condensation is due to a unique necklace-like structure of the hydrophobic polyelectrolytes. The beads on the necklace are dense hydrophobic domains with very low concentration of the solvent molecules or even completely "dry" globules. The exclusion of the solvent from the interior of the beads changes completely the dielectric properties of the medium. Effectively the dielectric permittivity changes from that for water, $\varepsilon \approx 78$, at the bead surface to about $\varepsilon = 2.5$ inside "dry" beads. This dramatic change of the local dielectric constant enhances the counterion condensation, trapping condensed counterions inside beads and favoring the distribution of the ionized groups on the bead surface.

Unfortunately, the current models of polyelectrolytes in poor solvents[12,15−19] as well as computer simulations[29−36] completely ignore effect of the distribution of the solvent on the structure of polyelectrolyte chains by treating the solvent as a dielectric continuum. The detailed molecular dynamics simulations of polyelectrolyte systems with explicit solvent[40−42] were limited to the systems of short chains and addressed the problem of polyelectrolyte chain solvation and elucidated the effect of the ion size and valence on the counterion condensation on polyelectrolyte oligomers. In this paper we use detailed molecular dynamics simulations to study a collapse transition of model NaPSS chains in dilute solutions of polyelectrolytes in water at room temperature as a function of the chain's degree of sulfonation and degree of polymerization. The rest of the paper is organized as follows. In section 2 we describe simulation details. Section 3 presents our results on the dependence of the chain conformation on the fraction of the ionized groups, on the chain's degree of polymerization, and on distribution of the condensed counterions. Finally, in section 4 we summarize our results.

2. Simulation Details

We have performed molecular dynamics simulations of poly(styrene)-*co*-styrene sodium sulfonate (NaPSS) chains with the degree of polymerization $N = 16-64$ and fraction of the sulfonated groups $f = 0.25$, 0.33, 0.5, and 1 corresponding to every fourth, every third, every second, and every styrene group being sulfonated. The actual values of the fraction of charged monomers f_a are given in Table 1. We performed two sets of simulations with and without explicit solvent. In simulations with explicit solvent (water), the water molecules were modeled by the TIP3-PME model.[43] To model a polystyrene sulfonate chain, we used a combination of the united atom model and the all atomistic representation. The united atom model was used for the chain backbone, while the all atomistic representation was used for the benzene ring and styrene sulfonate part of the repeat unit (see Figure 1). The united atom model for the backbone was based on the force field developed by Wiener et al.,[44] Yang et al.,[45] and Mondello et al.[46] The AMBER 94 force field parameters were used for the atomistic model of the benzene ring. The interaction parameters and partial charge distribution for the sulfonated benzene ring were taken from Jang et al.[47] and supplemented by the generalized AMBER force field (GAFF).[48]

The total potential energy of the system consisted of the bonded, bond angle, dihedral angle, improper angle, and nonbonded interaction potentials:

$$U_{\mathrm{TOTAL}} = \sum_{\mathrm{BONDS}} K_r(r - r_{\mathrm{eq}})^2 + \sum_{\mathrm{ANGLES}} K_\theta(\theta - \theta_{\mathrm{eq}})^2 + \sum_{\mathrm{DIHEDRALS}} \frac{V_n}{2}[1 + \cos(n\phi - \gamma)] + \sum_{\mathrm{IMPROPER}} K_\chi(\chi - \chi_{\mathrm{eq}})^2 + \sum_{i<j}\left[\frac{A_{ij}}{R_{ij}^{12}} - \frac{B_{ij}}{R_{ij}^{6}} + \frac{q_i q_j}{\varepsilon R_{ij}}\right] \quad (1)$$

The interaction parameters for the van der Waals potential between heterogeneous atomic pairs were calculated as the geometric mean of the interaction parameters for each atom. The default AMBER force field weighing coefficients for pairwise energy and force contributions were used to account for contributions from the van der Waals and electrostatic interactions. The force field parameters are summarized in Table 2.

The simulations were performed using LAMMPS code.[49] The equations of motion were integrated by using the velocity Verlet algorithm with a time step of 1.0 fs. The bonds and angles of the TIP3P-PME water molecules were maintained by implementing the SHAKE algorithm. A Nose−Hoover thermostat and barostat with relaxation times of 0.1 and 1.0 ps respectively were used to maintain temperature and pressure in a system. The system was periodic in the x, y, and z directions. The standard Ewald summation method with accuracy 1.0×10^{-6} and the near-field cutoff set to 15.0 Å was used to account for

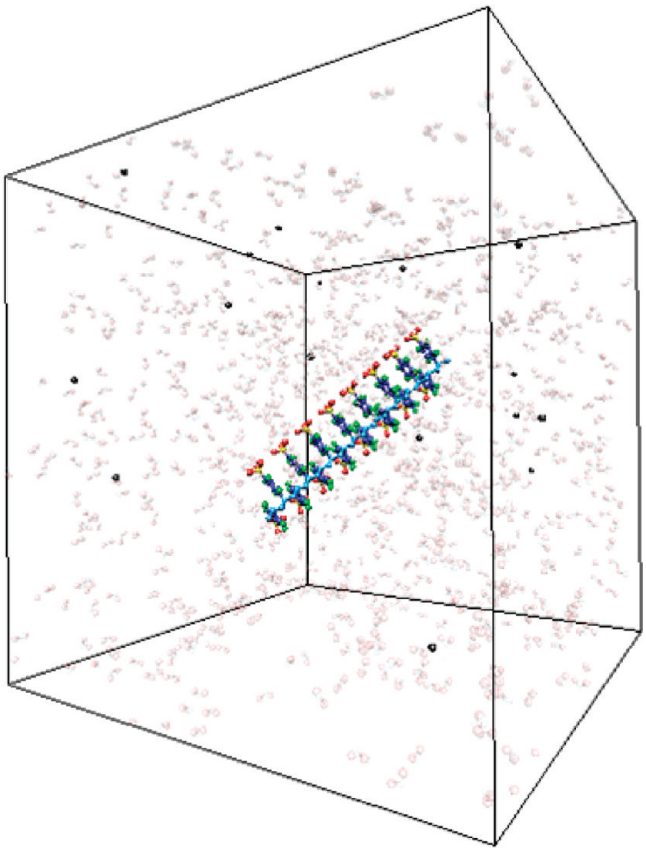

Figure 2. Snapshot of the initial system configuration.

contributions from the long-range electrostatic interactions during NPT ensemble simulations, and the PPPM method was used for the NVT simulations. Each simulation run consisted of two simulation steps: (1) NPT MD simulation, for relaxation of the initial system configuration to achieve an equilibrium box size; and (2) NVT MD simulation to obtain the equilibrium chain configurations and counterion distribution. At the beginning of the first simulation step a PSS chain was placed along the diagonal of a cubic simulation box. TIP3P-PME water molecules and Na^+ counterions were randomly distributed over the volume of the simulation box. Figure 2 shows the snapshot of the initial system configuration. The system was relaxed for 10 ns to achieve the equilibrium box volume, average system pressure (1 atm), and temperature of 300 K. The pressure and temperature control during this simulation step was achieved by using a Nose−Hoover barostat and thermostat. The final simulation box size was selected in such a way to have a polymer concentration close to 1.0 mol/L. (The simulation box sizes and the number of atoms in a system are given in Table 1.) This simulation run followed by constant volume simulations lasting 50 ns, with the last 10 ns used for the data analysis. During this simulation step the temperature was controlled by using the Nose−Hoover thermostat.

In addition to the molecular dynamics (MD) simulations with explicit solvent, we performed NVT ensemble simulations of the NaPSS chain in a dielectric continuum with a dielectric permittivity 77.73 corresponding to water at 300 K.[50] The temperature control in these simulations was achieved by coupling the system to a Langevin thermostat with a damping constant set to 0.01 fs^{-1}. The simulation box sizes for these simulations are shown in Table 1. The duration of these simulation runs was up to 100 ns for the longest chains. To verify that the system reached an equilibrium, we performed simulations starting from different initial conditions. Since we used three-dimensional periodic boundary conditions, our simulations correspond to dilute polyelectrolyte solutions.

3. Simulation Results

Figure 3 shows snapshots of the typical chain conformations as a function of the chain degree of polymerization N and degree of sulfonation f. Polymer chains with degree of polymerization $N = 16$, 32, and 64 with the sulfonation degree $f = 0.25$ and 0.33 form dense globule-like structures. (Here and below in the text we use the fractions of charged monomers $f = 1$, 0.5, 0.33, and 0.25 to specify that every, every second, every third, and every fourth monomer was charged. The actual values of the fraction of charged monomers f_a are listed in Table 1. For the short chains the actual fraction of charged monomers f_a can deviate from f due to finite chain length and charge distribution.) The charged sulfonate groups are located on the surface of the globule, thus allowing the water molecules to form hydration cages around charges. With increasing the degree of sulfonation to $f = 1/2$, polystyrene sulfonate chains form more open structures. For the short chains with the degree of polymerization $N = 16$ a chain has a horseshoe-like configuration with all styrene sulfonate groups located on the outer surface of a shoe while hydrophobic benzene rings of the styrene groups form the inner part of the horseshoe. This conformation optimizes the hydrophobic attraction between benzene rings and the electrostatic repulsion between charged sulfonate groups. The collapsed structure of a chain persists for polystyrene sulfonate chains with the degree of polymerization $N = 32$ and sulfonation degree $f = 1/2$. However, a longer polystyrene sulfonate chain with $N = 64$ and $f = 1/2$ adopts a tadpole configuration. This peculiar change in the chain structure indicates the existence of a transition between collapsed and stretched chain conformations with increasing the fraction of the charged groups on the polymer backbone. Note that this sudden change in the chain conformation is in agreement with the coarse-grained MD simulations of a polyelectrolyte chain in poor solvent conditions for the polymer backbone.[12] The fully sulfonated polystyrene chains have elongated conformations with the chain's end-to-end distance being close to R_{max}, the size of the carbon backbone in the all-trans conformation. Note that we only report simulations of a fully sulfonated chain with the degree of polymerization $N = 16$ in explicit solvent. For the longer chains with $N = 32$ and 64 the chain size is larger than the size of the simulation box. In this case the interactions with the chain's periodic images result in chain folding. To study conformations of the fully sulfonated chains, we performed simulations of NaPSS chains in the larger simulation box without explicit solvent (see Table 1). The simulations with explicit solvent for these box sizes will be prohibitively long.

To quantify the effect of the chain degree of sulfonation and polymerization degree on the chain configuration, in Figure 4 we show dependence of square root of the mean square average radius of gyration of the polystyrene sulfonate chains. In our calculations of the mean square average value of the radius of gyration, we assign equal weights to all atoms on the polymer chain:

$$\langle R_g^2 \rangle = \frac{1}{N_{chain}} \left\langle \sum_{i=1}^{N_{chain}} (\vec{R}_i - \vec{R}_{cm})^2 \right\rangle \qquad (2)$$

where $\vec{R}_{cm}$ is the radius vector of the chain's center of mass. The dependence of the chain size on the degree of polymeri-

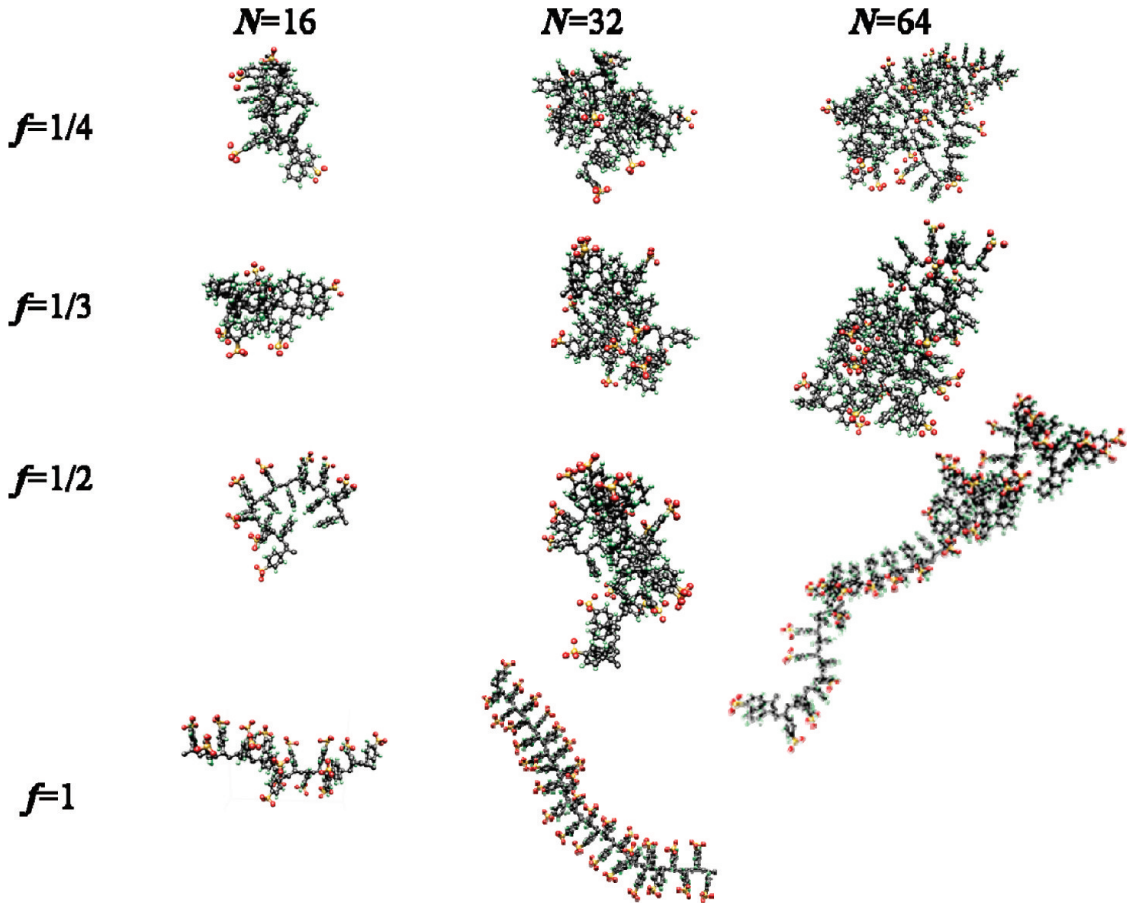

Figure 3. Snapshots of polystyrene sulfonate chains from simulations with explicit water and in a dielectric medium ($f = 1$, $N = 32$). The oxygen atoms are shown in red, hydrogen atoms are colored in cyan, carbon atoms are shown in gray, and sulfur atoms are shown in yellow.

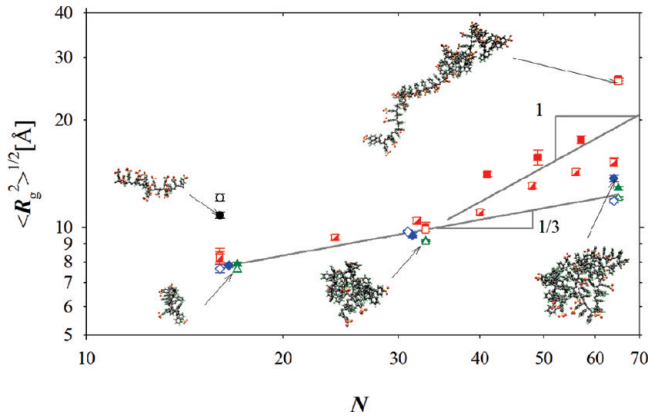

Figure 4. Dependence of the square root of the mean square average radius of gyration $\langle R_g^2\rangle^{1/2}$ on the degree of polymerization N for polystyrene sulfonate chains with the degree of sulfonation f: $f = 1.0$ (circles), $f = 0.5$ (squares), $f = 0.333$ (rhombs), and $f = 0.25$ (triangles). Filled symbols represent simulations with explicit water; half-filled and open symbols correspond to simulations in a medium with dielectric constant $\varepsilon = 77.73$ and monomer number density 6×10^{-4} and 8×10^{-6} Å^{-3}, respectively. The solid lines have slopes of 1/3 and 1, and are shown to illustrate two different scaling regimes. Insets show typical chain conformations.

zation supports our previous observation that polystyrene sulfonate chains with the degree of polymerization $N = 16$, 32, and 64 and sulfonation degree $f = 0.33$ and 0.25 form a globule-like structure. In a globule conformation the chain's size $R \propto \langle R_g^2\rangle^{1/2}$ scales with the chain degree of polymerization as $N^{1/3}$. It is interesting to point out that simulations both with and without explicit solvent lead to close values of the chain sizes in the collapsed chain regime. The change in the chain size is observed for polystyrene sulfonate chain with the sulfonation degree $f = 1/2$ and degree of polymerizations $N = 41-64$ in comparison with a chain consisting of $N = 32$ repeat units. This transformation in the chain size scaling is an indication of the Rayleigh instability of a charged polymeric globule. The charged polymeric globule is stable as long as the globule surface energy F_{surf} of a globule with the interfacial energy γ and size R, $F_{surf} \approx \gamma R^2$, is larger than the energy of the electrostatic interactions between charged groups $F_{elec} \approx k_B T l_B (fN)^2/R$, where l_B is the Bjerrum length—the length scale at which the electrostatic interaction between two elementary charges e in a medium with the dielectric constant ε is equal to the thermal energy $k_B T$. The charged globule becomes unstable when the globule electrostatic energy exceeds the surface energy, $F_{elec} > F_{surf}$. Thus, the critical value of the fraction of charged monomers (sulfonation degree) which separates the stable globule regime from the unstable one can be obtained by equating the surface and electrostatic energies, $F_{surf} \approx F_{elec}$, and solving this equation for the parameter f:

$$f_{crit} \propto \sqrt{R^3/N^2} \propto 1/\sqrt{N} \tag{3}$$

Figure 5 shows the dependence of the reduced chain size $\langle R_g^2\rangle^{1/2}/N^{1/3}$ as a function of the normalized charge $Q/Q_{crit} = fN/f_{crit}N \propto f\sqrt{N}$. As expected, the data points collapsed into a universal plot. There is a striking similarity between these results and the results of the coarse-grained simulations which also show a transition between collapsed and elongated chain states.

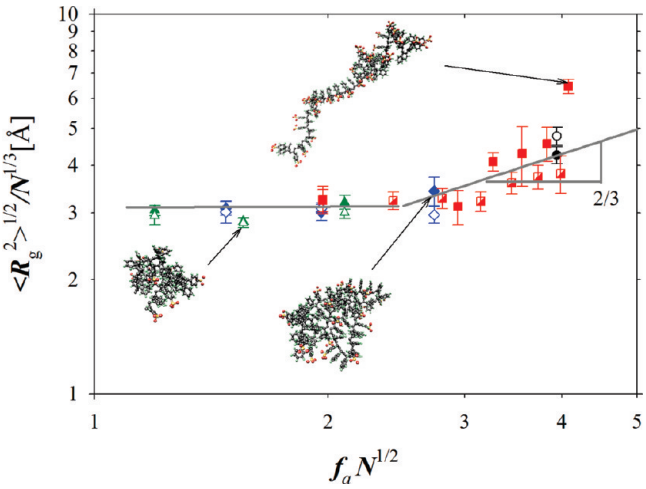

Figure 5. Dependence of the reduced chain size $\langle R_g^2\rangle^{1/2}/N^{1/3}$ on the reduced chain charge $f_aN^{1/2}$ for polystyrene sulfonate chains with the degree of sulfonation f: $f = 1.0$ (circles), $f = 0.5$ (squares), $f = 0.333$ (rhombs), and $f = 0.25$ (triangles). Filled symbols represent simulations with explicit water; half-filled and open symbols correspond to simulations in a medium with dielectric constant $\varepsilon = 77.73$ and monomer number density 6×10^{-4} and 8×10^{-6} Å^{-3}, respectively. Insets show typical chain conformations. The lines on this plot are not the best fits: they illustrate two different scaling regimes.

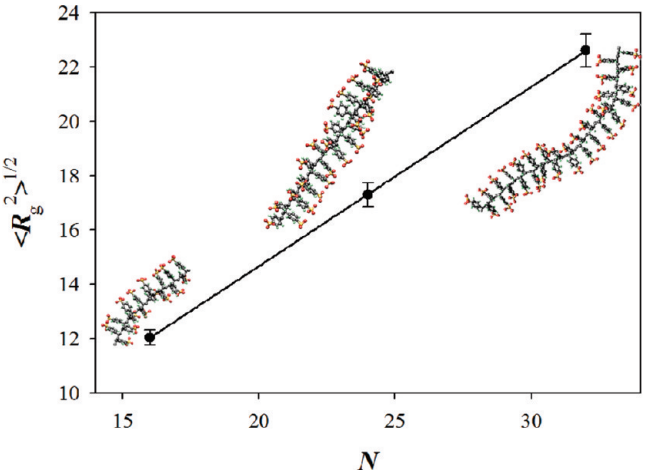

Figure 6. Dependence of the square root of the mean square average radius of gyration $\langle R_g^2\rangle^{1/2}$ for chains of fully sulfonated polystyrene sulfonate chains ($f = 1.0$) on the chain's degree of polymerization N obtained from simulations in a medium with dielectric constant $\varepsilon = 77.73$ and monomer number density 8×10^{-6} Å^{-3}.

Thus, coarse-grained simulations[12] provide a qualitatively correct picture of the stability of the charged polymeric globule. Note that a transition is observed for simulations both with and without explicit solvent. However, the location of the transition is shifted to the larger chain charge values for simulations without explicit solvent, indicating a slightly stronger monomer−monomer attraction.

Fully sulfonated chains behave differently from the partially sulfonated ones. They all have a stretched conformation. Unfortunately, we have only been able to perform simulations of the shortest polystyrene sulfonate chain with the degree of polymerization $N = 16$ in water. To establish the chain size scaling for the fully sulfonated chains, we have performed simulations of the NaPSS chains in a dielectric continuum (see Table 1). In Figure 6 we show dependence of the square root of the mean square average radius of gyration $\langle R_g^2\rangle^{1/2}$ for chains with the degree of sulfonation $f = 1$ as a function of the chain's degree of polymerization N. All chains follow the expected linear scaling dependence of the chain size on the degree of polymerization, $\langle R_g^2\rangle^{1/2} \propto N$.

Information about charged group distribution in polystyrene sulfonate globules can be obtained from the radial distribution function $g(r)_{S-S}$ between sulfur atoms of the SO_3^- group. Figure 7 shows this correlation function for partially sulfonated chains with $f = 1/3$ and degrees of polymerization $N = 16$, 31, and 64. For all chains there are two characteristic peaks. The first peak is located at about 6−8 Å distance, which is a distance between closest charged groups on the surface of the globule. The second peak located at larger distances represents correlations between charged groups located at the opposite sides of the globule. This form of the correlation function also indicates that the charged groups are preferentially located on the surface of the globule. There are two effects that can lead to such charge distribution. The first one is associated with the formation of the hydration cage by water molecules around the SO_3^- group. The second effect is due to electrostatic repulsion between similar charged groups. The minimum of the electrostatic energy is achieved when the charged groups are located on the surface of the globule. The second effect seems to be the dominant one since simulations both with and without explicit solvent lead to close values of the size of the globule. To see how many water molecules are inside the globule and to establish the correlation between distribution of the charged groups and water in Figure 8, we show the radial density profile of the water molecules with respect to the globule center of mass. The water molecules are excluded from the core of the globule. The polymer−water interface is sharper for shorter chains independent of their degree of sulfonation. For longer chains we see a much more gradual increase in the water density. This is due to globule asymmetry. The larger globules have an ellipsoidal shape.

The most striking difference that separates two simulations is the distribution of the counterions around the polymer backbone. For simulations with explicit water there are peaks located at 4, 6, and 8 Å from the sulfur atom of the SO_3^- group (see Figure 9). These peaks appear due to formation of the solvation cages of water molecules around SO_3^- groups and sodium counterion. (The secondary peaks are due to correlations between a sodium ion and neighboring along the polymer backbone SO_3^- groups.) For the polyelectrolyte chain in a dielectric continuum there is only one broad peak, indicating the absence of the structural restrictions on the counterion location. A similar pattern in counterion distribution persists even for the collapsed chains. To illustrate this point in Figure 10, we show the radial distribution function for polystyrene sulfonate chains at different degrees of sulfonation. Even for partially sulfonated chains one can clearly identify two major peaks located at 4 Å and at about 6 Å distances. Insets in Figure 10 show locations of the sodium ions that result to such a form of the correlation function.

Small-angle neutron scattering (SANS) and small-angle X-ray scattering (SAXS) techniques are used to analyze the chain structure in solutions. In dilute solutions the scattering is dominated by the single chain contribution, and both techniques measure the single chain form factor

$$P(q) \approx \frac{1}{N_{\text{chain}}^2}\left\langle \sum_{i,j} \exp(i\vec{q}\cdot\vec{r}_{ij})\right\rangle \tag{4}$$

where $\vec{q}$ is the wave vector, $\vec{r}_{ij}$ is the radius vector between the ith and jth atoms on the chain, and the brackets $\langle\ \rangle$ denote the

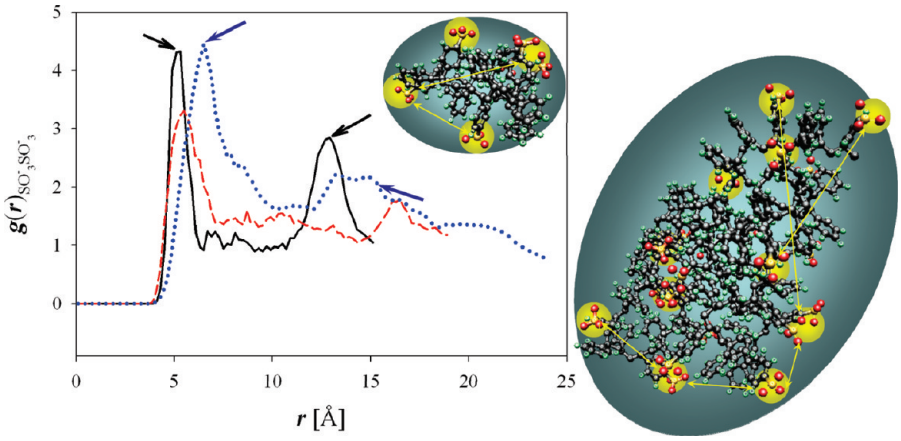

Figure 7. Radial distribution function of the sulfur atoms in the sulfonate group, $g(r)_{S-S}$, obtained from simulations with explicit water for polystyrene sulfonate chains with the sulfonation degree $f = 1/3$ and degree of polymerization $N = 16$ (solid line), $N = 31$ (dashed line), and $N = 64$ (dotted line). Arrows and insets indicate the location of the peak and the corresponding distances between sulfur atoms which contribute to these peaks. The smaller inset shows a chain with the degree of polymerization $N = 16$, and the larger inset is for the chain with $N = 64$.

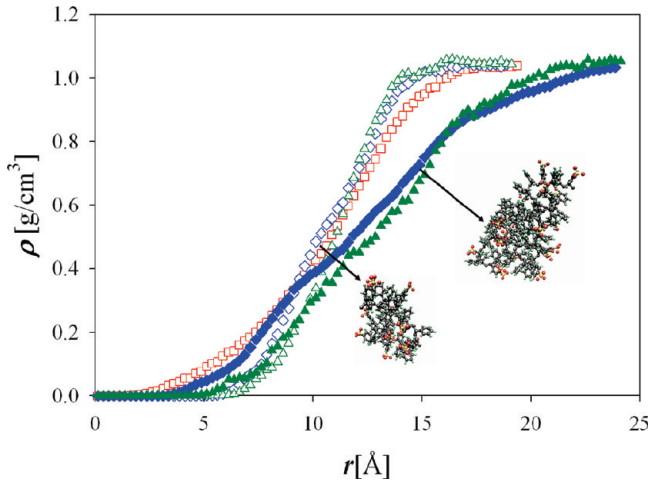

Figure 8. Density distribution function of water obtained from simulations of NaPSS chains with $N = 33$ and $f = 0.5$ (red open squares), $N = 31$ and $f = 0.333$ (blue open rhombs), $N = 33$ and $f = 0.25$ (green open triangles), $N = 64$ and $f = 0.333$ (blue filled rhombs), and $N = 65$ and $f = 0.25$ (green filled triangles).

ensemble average over chain conformations. In writing eq 4 we have assumed that all atoms have similar scattering amplitudes.

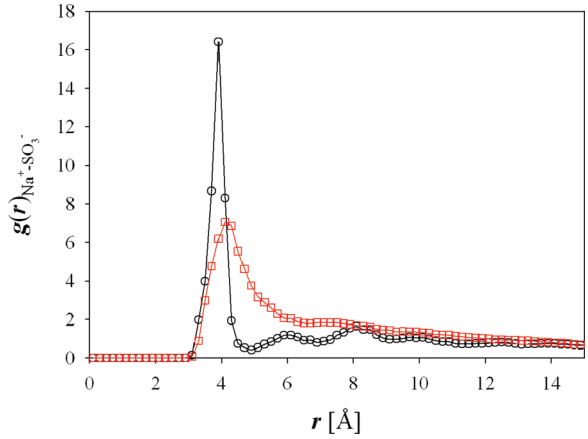

Figure 9. Radial distribution function of Na^+ and S atom in the sulfonate group $g(r)_{Na^+-SO_3^-}$ for simulations with degree of polymerization $N = 16$ and degree of sulfonation $f = 1.0$. Circles represent the distribution function obtained in simulations with explicit water, and squares show the distribution function for simulations in a dielectric medium.

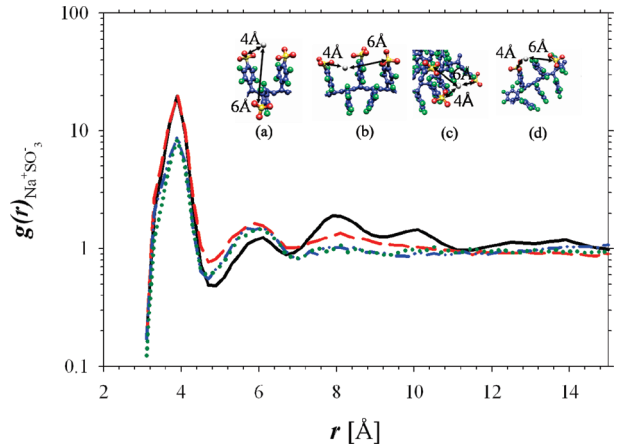

Figure 10. Radial distribution function of Na^+ and S atom in the sulfonate group $g(r)_{Na^+-SO_3^-}$ for simulations with explicit water for systems with $N = 16$ and $f = 1$ (solid line), $N = 16$ and $f = 0.5$ (dashed line), $N = 16$ and $f = 0.333$ (dash−dot−dot line), and $N = 17$ and $f = 0.25$ (dotted line). Inset shows the corresponding distances where the peaks at 4 and 6 Å are located for the chains with different fractions of sulfonation: $f = 1.0$ (a), $f = 0.5$ (b), $f = 0.333$ (c), and $f = 0.25$ (d).

Figure 11 shows the single chain form factor from our simulations which was calculated by using only carbon atoms

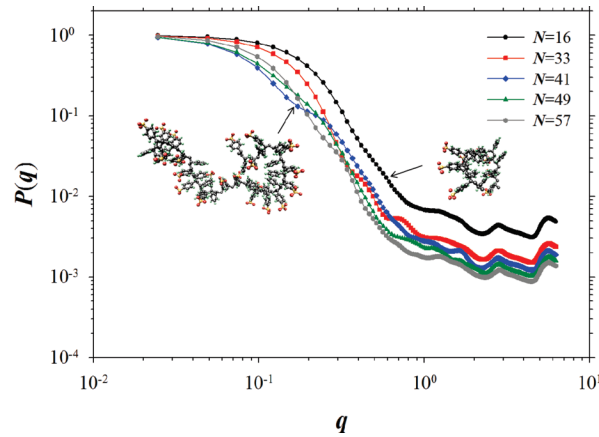

Figure 11. Form factor of the polystyrene sulfonate chains with the degree of sulfonation $f = 0.5$ obtained from simulations with explicit solvent.

TABLE 2: Force Field Parameters

van der Waals Parameters				
atom type	description	$R^{*\,a,c}$ (Å)	$\varepsilon^{b,c}$ (kcal/mol)	mass (au)
C3	sp^3 carbon with three hydrogens[45]	2.0580	0.1494	15.034
C1	sp^3 carbon with one hydrogen[45]	1.9580	0.0994	13.018
C2	sp^3 carbon with two hydrogens[45]	2.0580	0.1094	14.026
CA	aromatic carbon[51]	1.908	0.0860	12.011
H	hydrogen attached to an aromatic carbon[51]	1.4590	0.0150	1.008
S	sulfur in sulfonate group[47]	2.015	0.3440	32.06
O_S	oxygen in sulfonate group[47]	1.7023	0.0957	15.9994
Na	sodium counterion[47]	1.572	0.5	22.98977
H_{water}	hydrogen in water[43]	0.0	0.0	1.008
O_{water}	oxygen in water[43]	1.7683	0.102	15.9994

Bond Parameters		
bond	K_r (kcal/mol Å^2)	r_{eq} (Å)
C−C[51]	310.0	1.526
C−CA[51]	317.0	1.510
CA−CA[51]	469.0	1.400
CA−H[51]	367.0	1.080
CA−S[47]	350.0	1.740
S−O[47]	350.0	1.480

Angle Parameters		
bond	K_θ (kcal/mol rad^2)	θ_{eq} (deg)
C2−C1−C2[46]	60.0	109.47
C1−C2−C1[46]	63.0	109.47
C−C−CA[46]	60.0	109.47
C−CA−CA[46]	70.0	120.0
CA−CA−S[d,46]	70.0	120.0
O_S−S−O_S[47]	175.0	115.50
CA−CA−CA[51]	63.0	120.0
CA−CA−H[51]	35.0	120.0

Dihedral Parameters			
dihedral	$K_\phi{}^e$ (kcal/mol rad^2)	d^e	n^e
X−C−C−X[f,46]	1.4	1	3
CA−CA−CA−CA[51]	3.625	−1	2
CA−CA−CA−X[f,51]	3.625	−1	2
X−S−CA−CA[f,48]	1.3	−1	2

Improper Torsion Parameter		
improper dihedral	K_χ (kcal/mol)	χ_{eq} (deg)
phenyl ring torsion around C−CA[g]	2.0[46]	180
to maintain the stereochemical configuration of aliphatic CH[h]	50.0[46]	125.04

[a] van der Waals radius R_i^* for a given atom in Å. The value of van der Waals diameter used for the interaction potential (see eq 1) between atoms i and j is equal to $R_{ij}^* = R_i^* + R_j^*$. [b] van der Waals interaction parameter for a given atom in kcal/mol. The values of the van der Waals interaction parameter used for the interaction potential (see eq 1) between atoms i and j is equal to $\varepsilon_{ij} = (\varepsilon_i\varepsilon_j)^{1/2}$. [c] Note that $A_{ij} = \varepsilon_{ij}(R_{ij}^*)^{12}$ and $B_{ij} = 2\varepsilon_{ij}(R_{ij}^*)^6$. [d] This assumes that S behaves as C1 attached to CA. [e] The dihedral potential energy, $(V_n/2)[1 + \cos(n\phi - \gamma)]$ is converted to $K_\phi[1 + d\cos(n\phi)]$ such that it is compatible with the LAMMPS definition. [f] X denotes any atom type. [g] We approximated the improper dihedral potential for phenyl ring rotation $K_\chi \cos^2(\chi - \pi/2)$ with $K_\chi = 2.0$ kcal/mol given in ref 46 by $K_\chi(\chi - \pi)^2$ used in LAMMPS. This approximation does not lead to significant differences in rotational configurations of a phenyl group corresponding to exact and approximated potentials because its structure is invariant with respect to transformation $0 \rightarrow \pi$ for the dihedral angle. [h] This potential is introduced to maintain sp^3 configuration of the bonds around aliphatic carbon in the united atom representation of the chain backbone and to prevent the collapse of four carbons, C_1, C_3, $C_{1'}$, and C_2 into a plane, where C_1, C_2, and $C_{1'}$ are backbone carbon atoms, and the C_2−C_3 bond connects the phenyl group to the backbone (see ref 46 for details). The equilibrium value of the angle between normal vectors to the planes ($C_{1'}$,C_2,C_1) and (C_1,C_2,C_3) is equal to $\chi_{eq} = 125.04°$.

and setting the scattering amplitudes to unity. For short chains with $N < 41$ we have a gradual monotonic decrease in the scattering intensity with increasing q. For these degrees of polymerizations a NaPSS chain forms a globule. However, for the chains with degrees of polymerization $N \geq 41$, we begin to see shoulders to appear in the small q window. These shoulders are manifestations of the internal chain organizations. Indeed for these chain degrees of polymerization we observed an increase in a chain size (see Figure 5). The insets of the typical chain conformations shown in Figure 11 demonstrate that the chain has a tadpole-like configuration. One can assign a shoulder to the monomer−monomer correlations between the "head" and "tail" of the tadpole.

4. Conclusions

We presented results of the molecular dynamics simulations of sodium polystyrene sulfonate in salt-free aqueous solutions.

Our simulations showed that polyelectrolyte chains with a charge smaller than the critical charge Q_{crit} collapse, forming dense globules (see Figure 5). The value of the critical charge is determined by the Rayleigh stability condition that is the result of optimization of the globule surface energy and energy of the electrostatic repulsion between charged groups. Increasing the charge asymmetry beyond the critical value Q_{crit} leads to chain elongation. For example, an NaPSS chain in water with the degree of polymerization $N = 64$ and degree of sulfonation $f = 0.5$ forms a tadpole (see Figure 3).

The ionized groups were found to be located on the surface of the globule. The placement of the charged groups on the surface of the globule reduces the energy of the electrostatic repulsion between them and also allows formation of the water solvation cages around charged groups. Note that this location of the charged groups could be one of the reasons for the peculiar concentration dependence of the osmotic pressure of salt-free NaPSS solutions.[37]

The most striking difference between simulations with the explicit solvent and ones in which the water was modeled by a dielectric continuum is in the counterion distribution functions. In the case of the simulations with explicit water the correlation function of the sodium ions Na^+ and SO_3^- groups has multiple peaks, indicating the strong effect of the surrounding water molecules on the counterion distribution around the polymer backbone.

Acknowledgment. This work was supported by the Donors of the American Chemical Society Petroleum Research Fund under Grant PRF 44861-AC7.

References and Notes

(1) Oosawa, F. *Polyelectrolytes*; Marcel Dekker: New York, 1971.
(2) Forster, S.; Schmidt, M. *Adv. Polym. Sci.* **1995**, *120*, 51.
(3) Mandel, M. In *Encyclopedia of polymer science and engineering*; Wiley: New York, 1988.
(4) Hara, M. *Polyelectrolytes*; Marcel Dekker: New York, 1993.
(5) Barrat, J. L.; Joanny, J. F. *Adv. Chem. Phys.* **1996**, *94*, 1.
(6) Dobrynin, A. V.; Rubinstein, M. *Prog. Polym. Sci.* **2005**, *30*, 1049.
(7) Dobrynin, A. V. *Curr. Opin. Colloid Interface Sci.* **2008**, *13*, 376.
(8) Grosberg, A. Y.; Khokhlov, A. R. *Statistical Physics of Macromolecules*; AIP Press: New York, 1994.
(9) Rubinstein, M.; Colby, R. H. *Polymer Physics*; Oxford University Press: New York, 2003.
(10) Doi, M.; Edwards, S. F. *The theory of polymer dynamics*; Oxford University Press: New York, 1986.
(11) Rayleigh, L. *Philos. Mag.* **1882**, *14*, 184.
(12) Dobrynin, A. V.; Rubinstein, M.; Obukhov, S. P. *Macromolecules* **1996**, *29*, 2974.
(13) Chodanowski, P.; Stoll, S. *J. Chem. Phys.* **1999**, *111*, 6069.
(14) Lyulin, A. V.; Dunweg, B.; Borisov, O. V.; Darinskii, A. A. *Macromolecules* **1999**, *32*, 3264.
(15) Solis, F. J.; de la Cruz, M. O. *Macromolecules* **1998**, *31*, 5502.
(16) Balazs, A. C.; Singh, C.; Zhulina, E.; Chern, S. S.; Lyatskaya, Y.; Pickett, G. *Prog. Surf. Sci.* **1997**, *55*, 181.
(17) Migliorini, G.; Lee, N.; Rostiashvili, V.; Vilgis, T. A. *Eur. Phys. J. E* **2001**, *6*, 259.
(18) Dobrynin, A. V.; Rubinstein, M. *Macromolecules* **2001**, *34*, 1964.
(19) Dobrynin, A. V.; Rubinstein, M. *Macromolecules* **1999**, *32*, 915.
(20) Aseyev, V. O.; Klenin, S. I.; Tenhu, H.; Grillo, I.; Geissler, E. *Macromolecules* **2001**, *34*, 3706.
(21) Lee, M. J.; Green, M. M.; Mikes, F.; Morawetz, H. *Macromolecules* **2002**, *35*, 4216.
(22) Essafi, W. Ph.D. Thesis, Paris, 1996.
(23) Essafi, W.; Spiteri, M. N.; Williams, C.; Boue, F. *Macromolecules* **2009**, *42*, 9568.
(24) Heitz, C.; Rawiso, M.; Francois, J. *Polymer* **1999**, *40*, 1637.
(25) Waigh, T. A.; Ober, R.; Williams, C. E.; Galin, J. C. *Macromolecules* **2001**, *34*, 1973.
(26) Baigl, D.; Sferrazza, M.; Williams, C. E. *Europhys. Lett.* **2003**, *62*, 110.
(27) Qu, D.; Baigl, D.; Williams, C. E.; Mohwald, H.; Fery, A. *Macromolecules* **2003**, *36*, 6878.
(28) Bordi, F.; Cametti, C.; Gili, T.; Sennato, S.; Zuzzi, S.; Dou, S.; Colby, R. H. *J. Chem. Phys.* **2005**, *122*, 234906.
(29) Micka, U.; Holm, C.; Kremer, K. *Langmuir* **1999**, *15*, 4033.
(30) Micka, U.; Kremer, K. *Europhys. Lett.* **2000**, *49*, 189.
(31) Limbach, H. J.; Holm, C. *Comput. Phys. Commun.* **2002**, *147*, 321.
(32) Limbach, H. J.; Holm, C. *J. Phys. Chem. B* **2003**, *107*, 8041.
(33) Limbach, H. J.; Holm, C.; Kremer, K. *Macromol. Symp.* **2004**, *211*, 43.
(34) Liao, Q.; Dobrynin, A. V.; Rubinstein, M. *Macromolecules* **2006**, *39*, 1920.
(35) Jeon, J.; Dobrynin, A. V. *Macromolecules* **2007**, *40*, 7695.
(36) Jeon, J.; Dobrynin, A. V. *J. Phys. Chem. B* **2006**, *110*, 24652.
(37) Essafi, W.; Lafuma, F.; Baigl, D.; Williams, C. E. *Europhys. Lett.* **2005**, *71*, 938.
(38) Manning, G. S. *J. Chem. Phys.* **1969**, *51*, 924.
(39) Manning, G. S. *Ber. Bunsen-Ges.: Phys. Chem. Chem. Phys.* **1996**, *100*, 909.
(40) Chialvo, A. A.; Simonson, J. M. *J. Phys. Chem. B* **2005**, *109*, 23031.
(41) Chialvo, A. A.; Simonson, J. M. *J. Mol. Liq.* **2007**, *134*, 15.
(42) Druchok, M.; Hribar-Lee, B.; Krienke, H.; Vlachy, V. *Chem. Phys. Lett.* **2008**, *450*, 281.
(43) Price, D. J.; Brooks, C. L. *J. Chem. Phys.* **2004**, *121*, 10096.
(44) Weiner, S. J.; Kollman, P. A.; Case, D. A.; Singh, U. C.; Ghio, C.; Alagona, G.; Profeta, S.; Weiner, P. *J. Am. Chem. Soc.* **1984**, *106*, 765.
(45) Yang, L.; Tan, C.-H.; Hsieh, M.-J.; Wang, J.; Duan, Y.; Cieplak, P.; Caldwell, J.; Kollman, P. A.; Luo, R. *J. Phys. Chem. B* **2006**, *110*, 13166.
(46) Mondello, M.; Yang, H.-J.; Furuya, H.; Roe, R.-J. *Macromolecules* **1994**, *27*, 3566.
(47) Jang, S. S.; Lin, S.-T.; Maiti, P. K.; Blanco, M.; Goddard, W. A.; Shuler, P.; Tang, Y. *J. Phys. Chem. B* **2004**, *108*, 12130.
(48) Junmei, W.; Romain, M. W.; James, W. C.; Peter, A. K.; David, A. C. *J. Comput. Chem.* **2004**, *25*, 1157.
(49) Plimpton, S. J. *J. Comput. Phys.* **1995**, *117*, 1.
(50) Anderson, G. S.; Miller, R. C.; Goodwin, A. R. H. *J. Chem. Eng. Data* **2000**, *45*, 549.
(51) Cornell, W. D.; Cieplak, P.; Bayly, C. I.; Gould, I. R.; Merz, K. M.; Ferguson, D. M.; Spellmeyer, D. C.; Fox, T.; Caldwell, J. W.; Kollman, P. A. *J. Am. Chem. Soc.* **1995**, *117*, 5179.

JP101978K